A new approach for drought forecasting using wavelet-ANN model and satellite images

Maedeh Behifar[a], Ata Abdollahi Kakroodi[a,*], Majid Kiavarz[a], Ghasem Azizi[b]

[a]Department of Remote Sensing and GIS, Faculty of Geography, University of Tehran, Tehran, Iran

[b]Department of Geography, Faculty of Geography, University of Tehran, Tehran, Iran

(Communicated by Hayder Akca)

Abstract

Forecasting drought is a challenging endeavor due to various underlying factors and mechanisms. Thus, the need for robust and precise forecasting models is paramount. In this study, a method that utilizes the wavelet neural network and spatial proximity data derived from satellite images to enhance the accuracy of drought forecasts is presented. This technique applies satellite-based precipitation and evapotranspiration data to calculate drought indices. It then uses the wavelet neural network approach to forecast drought intensity in different months of the subsequent year. To better discern random fluctuations from actual drought signals and enhance forecast accuracy, we utilize spatial proximity data from satellite images to forecast drought at the East Isfahan climate station. Our findings validate the capability of the wavelet neural network approach to forecast drought with a reasonable degree of accuracy. Also, leveraging neighboring data can potentially improve forecasting precision, as evidenced by a correlation of 0.675 between the target and predicted values.

Keywords: drought, forecasting, wavelet, artificial neural network, satellite image
2020 MSC: 68T07, 42C40

1 Introduction

Drought, a naturally recurring climate phenomenon, poses significant challenges to various sectors, including agriculture, energy, and transportation [28]. It ranks among the most devastating natural calamities [27]. The importance of drought forecasting lies in its ability to provide early warnings, aid risk management, and alleviate pressure on water resources [19, 21].

However, forecasting drought is complex due to its multiple mechanisms and influencing factors [18], underscoring the need for robust and accurate forecasting models [1, 12]. Current prediction strategies include statistical, dynamic, and hybrid methods [14, 24].

Artificial neural networks exhibit impressive proficiency in modeling and forecasting nonlinear time series. However, their prediction capacity for non-stationary data is constrained and dependent on the quality of data preprocessing [11].

---

*Corresponding author
   Email addresses: behifar.mh@ut.ac.ir (Maedeh Behifar), a.a.kakroodi@ut.ac.ir (Ata Abdollahi Kakroodi),
kiavarzmajid@ut.ac.ir (Majid Kiavarz), ghazizi@ut.ac.ir (Ghasem Azizi)

Wavelet transform enhances forecasting by decomposing the original time series into multiple resolutions. The effectiveness of hybrid wavelet-artificial neural network models for drought forecasting has been confirmed in several studies [6, 19].

The long-term periodic changes typical of drought require extensive data for accurate analysis. The inherent complexity of drought and data scarcity makes forecasting a challenge. The effects of drought often manifest in the stochastic component of the wavelet decomposition of drought series due to limited data length, rendering drought cycles difficult to discern.

There is a pressing need for a solution that can differentiate between random effects and drought signals in decomposed time series. Thus, we propose an approach that separates these elements in drought predictions derived from satellite imagery. This method incorporates spatial proximity data from satellite imagery to identify drought signals.

2 Materials and methods

2.1 Study area

In this study, drought was estimated in the location of the East Isfahan synoptic station. The region is subject to subtropical high pressure for more than half of the year, with most precipitation falling during the cold season. Isfahan has a dry, desert climate type with an average annual rainfall of 174 mm [23].

2.2 Data

Drought indices calculated from precipitation (TRMM 3B43) and evapotranspiration (PML) satellite products are used to forecast drought. A detailed description of the data and their specifications is presented in Table 1. Also, the precipitation data of the east Isfahan synoptic station is used as the reference data to calculate the target variable (SPI). The study period is between 2003 and 2017.

Table 1: Summary of the Remote Sensing data used in this study

Parameter	Satellite	Coverage		Resolution		Source
		Spatial	Temporal	Spatial	Temporal	
Evapotranspiration	Combined	$90°N-$ $-60°S$	2002-2019	500m	8-Day	[30]
Precipitation	TRMM and other source data	$50°N-$ $50°S$	1998-2019	$0.25°$	Monthly	[9]

2.3 Methods

2.3.1 Calculation of drought indices

According to the results of Behifar et al. [5], the ETCI and PCI drought indices were defined as appropriate indices for the study area. So, these indices were used to forecast the drought. The ETCI (Evapotranspiration Condition Index) and PCI (Precipitation Condition Index) were calculated by Equation (2.1) [5] and Equation (2.2) [31], respectively. The 6-month SPI (Standardized Precipitation Index) was selected as the target variable and was calculated by MATLAB code [4].

$$ETCI = \frac{ET_{i,j} - ET_{\min,j}}{ET_{\max,i} - ET_{\min,i}} \tag{2.1}$$

where, $ET_{i,j}$ is the actual evapotranspiration in the location i and time j. $ET_{\max,i}$ and $ET_{\min,i}$ are the maximum and minimum of actual evapotranspiration in location i during the study period, respectively.

$$PCI = \frac{P_{i,j} - P_{\min,j}}{P_{\max,i} - P_{\min,i}} \tag{2.2}$$

where, $P_{i,j}$ is the precipitation in the location i and time j. $P_{\max,i}$ and $P_{\min,i}$ are the maximum and minimum of precipitation in location i during the study period, respectively.

2.3.2 Drought forecasting

In this study, a wavelet neural network model has been applied to forecasts the drought. In this section, first, the method's theoretical basis is presented, and then then the implementation of the method is explained.

2.3.3 Wavelet neural network

In the wavelet neural network model, the input signal is first transformed into sub-signals by the wavelet technique. The extracted features are then fed as input to the neural network, and the neural network weights each feature according to its importance in generating the target signal.

The first step in wavelet transform is selecting the mother wavelet. A parent wavelet that can better fit the time series curve will provide better results.

Wavelets are defined as a family of functions obtained from the expansion and transmission of the mother wavelet. The function $\psi(t)$ is called the mother wavelet, and the daughter wavelet $\psi_{a,b}(t)$ is defined as Equation (2.3) [13].

$$\psi_{a,b}(t) = \frac{1}{\sqrt{a}} \psi\left(\frac{t-b}{a}\right) \tag{2.3}$$

where a is the scale parameter, and b is the shift that determines the position of the wavelet. Higher scales (longer wavelets) correspond with lower frequencies. There are different wavelet functions. Next, the most important step is the level of decomposition. The maximum decomposition levels can be estimated from Equation (2.4) [22].

$$l = Int[\log(N)] \tag{2.4}$$

The recommended decomposition level is represented by L, with N denoting the length of the time series. There are two categories of wavelet transforms: continuous and discrete. The function of Equation (2.5) mathematically outlines a continuous wavelet transform.

$$X_\omega(a,b) = \frac{1}{\sqrt{a}} \int_{-\infty}^{\infty} x(t)\bar{\psi}\left(\frac{t-b}{a}\right) dt \tag{2.5}$$

in this function, $\psi(t)$ is a continuous mother wavelet scaled by a factor a and propagated by a factor b. As scale and shift are continuous numbers, continuous transforms possess an infinite number of wavelets. In contrast, the discrete wavelet transform utilizes discrete values for scaling and shifting. The scale amplifies by powers of two, yielding $a = 1, 2, 4, ...$, while the shift factor increases as integers, meaning $b = 1, 2, 3, ...$.

Meteorologists, climatologists, and hydrologists often work with discrete-time signals rather than continuous time signals for practical applications. Notably, the discrete wavelet transform is discrete only in scale and offset, not in time. To accommodate discrete-time signals, wavelets must also be discrete in the time domain, which is referred to as discrete wavelet transforms in time.

According to Merry [20], the discrete wavelet transform operates as a filter bank. At each decomposition level, the original signal splits into two signals: approximation and detail. The approximation contains the low-frequency component, while the detail holds the high-frequency information of the original signal. This process continues as the decomposition level reaches its maximum, and the original signal eventually divides into multiple sub-signals. The depiction of the discrete wavelet transform as a filter bank is illustrated in Figure 1.
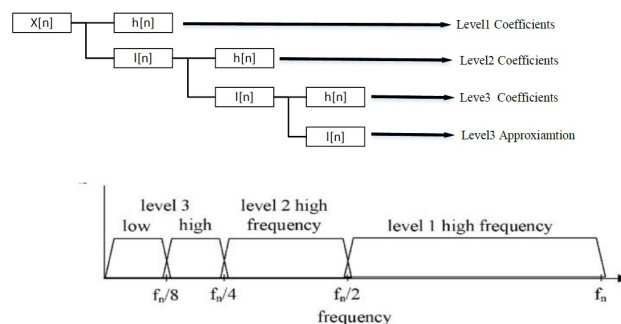

Figure 1: Diagram of the discrete wavelet transform as a filter bank.

After transforming the input signal, the next step is constructing a neural network. GMDH neural network is used in this study.

GMDH Neural Network

The Group method of data handling (GMDH) operates based on self-organized learning and forms a complex polynomial with high orders [2]. The GMDH algorithm is an inductive mechanism that extracts knowledge from data patterns. This method is particularly useful for complex systems and experimental data under conditions of uncertainty. When constructing a mathematical model to approximate an unfamiliar pattern of an object or process, this issue emerges [10]. One significant attribute of the GMDH is its ability to identify and eliminate redundant variables [2]. GMDH is often considered the pioneer of deep networks [25].

In the GMDH algorithm, the input-output relationship is approximated by nonlinear mapping through successive layers of neurons using polynomial functions. Given an input vector X, the goal is to predict an output that closely aligns with the target. Consequently, based on M observations of multi-input-single-output data pairs, Equation (2.6) is derived [26].

$$
\begin{aligned}
X &= (x_1, x_2, x_3, ..., x_N) \\
i &= 1, 2, 3, ..., M \\
y_i &= f(x_{i1}, x_{i2}, x_{i3}, ..., x_{in})
\end{aligned}
\tag{2.6}
$$

in this equation, X signifies the input data vector with N variables, M denotes the number of observations, y_i represents the target output, and f is the unknown function. To train the GMDH network to predict $\hat{y}_i$ with the input vector X, Equation (2.7) is utilized.

$$
\hat{y}_i = \hat{f}(x_{i1}, x_{i2}, x_{i3}, ..., x_{in})
\tag{2.7}
$$

where, $\hat{y}_i$ is the predicted output using the approximation function $\hat{f}$. The GMDH neural network needs to minimize the squared difference between the target and predicted values, so:

$$
Minimize: \qquad E = \sum_{i=1}^{M} (\hat{f}(x_{i1}, x_{i2}, x_{i3}, ..., x_{in}) - y_i)^2
\tag{2.8}
$$

The GMDH neural network employs the Kolmogorov-Gabor polynomial to map input and output variables, establishing a relation between M input variables and a single output variable as per Equation (2.9) [16].

$$
\hat{y} = a_0 + \sum_{i=1}^{m}(a_i x_i) + \sum_{i=1}^{m}\sum_{j=1}^{m}(a_{ij} x_i x_j) + \sum_{i=1}^{m}\sum_{j=1}^{m}\sum_{k=1}^{m}(a_{ijk} x_i x_j x_k) + ...
\tag{2.9}
$$

this equation can be rendered as a system of partial quadratic polynomials, each comprising only two variables (neurons), in the form of Equation (2.10).

$$
\hat{y} = G(x_i, x_j) = a_0 + a_1 x_i + a_2 x_j + a_3 x_i^2 + a_4 x_j^2 + a_5 x_i x_j
\tag{2.10}
$$

The main objective of GMDH is to ascertain the coefficients a_i in Equation (2.5), thereby minimizing the difference between the target and predicted output for each pair of input variables (x_i, x_j) [15, 16]. Hence, the least square error is leveraged in the form of Equation (2.11) to optimize the coefficients of each quadratic function.

$$
Minimize: \qquad E = \frac{\sum_{i=1}^{M}(\hat{y}_i - y_i)^2}{M}
\tag{2.11}
$$

In the basic form of the GMDH algorithm, all feasible combinations of two independent variables out of the total N input variables are applied to formulate the polynomial regression, as shown in Equation (2.5), which best fits the dependent variable. Consequently, in the first hidden layer of the neural network from observations (y_i, x_{ip}, x_{iq}), the number of neurons for different p and q is deduced from Equation (2.12).

$$
\binom{n}{2} = \frac{n(n-1)}{2} \qquad (p, q \in \{1, 2, 3, ..., n\})
\tag{2.12}
$$

So, for each triple M, the matrix of Equation (2.13) is given:

$$Y = Aa \tag{2.13}$$

where Y is the target vector, a is the vector of quadratic polynomial coefficients, and A is calculated as Equation (2.14):

$$Y = \{y_1, y_2, y_3, ..., y_M\}$$
$$a = (a_0, a_1, a_2, a_3, a_4, a_5)$$
$$A = \begin{bmatrix} 1 & x_{1p} & x_{1q} & x_{1p}x_{1q} & x_{1p}^2 & x_{1q}^2 \\ 1 & x_{2p} & x_{2q} & x_{2p}x_{2q} & x_{2p}^2 & x_{2q}^2 \\ \vdots & \vdots & \vdots & \vdots & \vdots & \vdots \\ 1 & x_{Np} & x_{Nq} & x_{Np}x_{Nq} & x_{Np}^2 & x_{Nq}^2 \end{bmatrix} \tag{2.14}$$

The least squares method produces a solution that is written as Equation (2.15):

$$a = (A^T A)^{-1} A^T Y \tag{2.15}$$

this equation calculates the vector of optimal coefficients for all M triples. It's worth noting that this procedure is reiterated for each neuron in the subsequent hidden layer according to the network connection topology. A standout feature of this network is that the neurons of the previous stage or layer are the producers of new neurons. To prevent network divergence, some of the generated neurons are removed [3].

2.4 Model implementation

Two strategies were assessed for drought forecasting. Initially, the competency of remote sensing indices was evaluated. Subsequently, the utility of adjoining information in the remote sensing data was inspected. The 6-month SPI was chosen as the benchmark for drought intensity.

In the first step, the 6-month SPI value at East Isfahan station was forecasted using ETCI and PCI indices via the wavelet neural network method from 2003 to 2016. The derived model was then used to predict the SPI in 2017. The input dataset was partitioned into training (70%) and testing (30%) segments.

Next, in the second step, three adjoining pixel values were utilized to model drought at the East Isfahan station. More precisely, pixel values located at the East Isfahan, Isfahan, and Kabutrabad synoptic stations were employed to predict the SPI time series. The target values in this phase were also the 6-month SPI of the East Isfahan station. This stage assumes that drought conditions (intensity, duration, and frequency) in a homogenous hydroclimatic unit are similar.

In the pixels of a hydroclimatic unit, components containing information will be analogous, while those housing noises (instantaneous and nonsystematic changes) will differ. Therefore, the components of information and noise can be more confidently separated.

A homogeneous hydroclimatic region refers to a collection of sub-regions bearing geographical similarities and similar hydrological responses [7]. That is, within a homogeneous hydroclimatic region, each hydrological and meteorological event is alike, and the basin exhibits a consistent response to these events [17].

Following this analysis, the subsequent steps were executed:

The first step in the wavelet transform involves selecting the mother wavelet and decomposition level. In this study, the Daubechies wavelet (db2) was chosen, and a decomposition level of three was applied, following an examination of different wavelet functions at five decomposition levels.

The subsequent step was the construction of a neural network. The GMDH model was chosen, featuring five layers with a maximum of 10 neurons per layer. The number of layers and neurons was determined via the trial-and-error method, and the best network was identified by comparing errors. A preference was given to the model's simplicity; thus, when errors were equal, the network with fewer neurons was selected. All the approximations and details extracted at the three decomposition levels were integrated into the neural network model, with the 6-month SPI introduced as the target.

Based on autocorrelation analysis, the optimal lags for drought forecasting were identified as one, two, and 12 months. For long-term forecasting purposes, lags of 12 and 24 months were applied, enabling the neural network model to predict the 12th month in advance.

3 Results and discussion

The capacity of remote sensing data for drought forecasting was assessed in two stages. Initially, remote sensing indices were evaluated for their ability to forecast drought. Subsequently, the benefit of incorporating spatial information to enhance forecast accuracy was explored.

3.1 First step

The db2 wavelet was applied to the ETCI and PCI indices at three decomposition levels, and the sub-signals were then employed as inputs for the neural network. This wavelet neural network model was implemented at the East Isfahan synoptic station, with results assessed against the station's 6-month SPI. Figures 2(a, b) display the neural network results on the training and validation datasets, while Figure 2(d) reveals the error histogram in the time series. Observed and predicted values in the training and validation datasets are depicted in Figure 3.
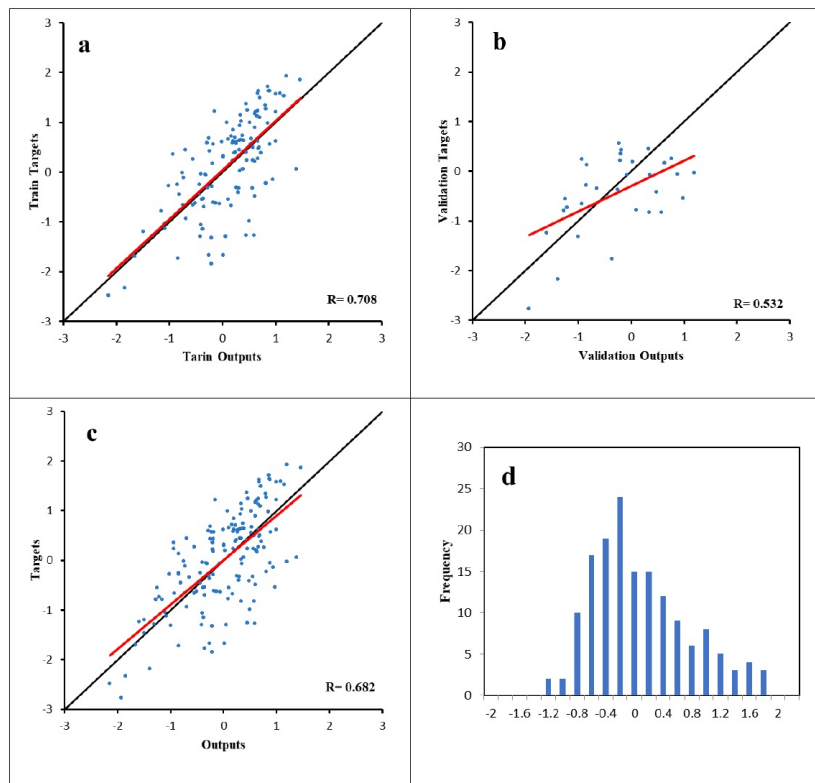

Figure 2: Neural network results in a) train dataset, b) validation dataset, c) All data, d) Error histogram of forecast
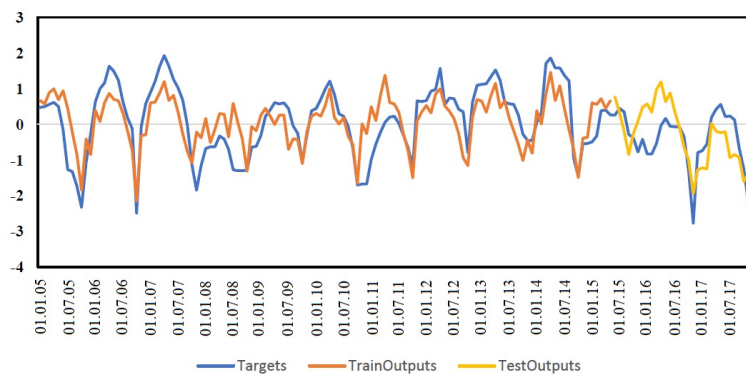

Figure 3: Time series of observed and predicted values in train and validation datasets.

As can be seen in Figure 2, model accuracy in the training and validation datasets was 0.708 and 0.532, respectively. It's worth noting that drought forecasting for each stage was performed 12 months in advance. The error distribution

displayed in Figure 2(d) indicates a relatively uniform distribution around zero, though the model does show a tendency to underestimate.

3.2 Second step

Wavelet transforms were applied to the ETCI and PCI indices at three locations (East Isfahan, Isfahan, and Kabutarabad station). All components extracted at three decomposition levels were used as input for the neural network model. In this stage, the wavelet type, decomposition level, and neural network parameters were used as in the previous stage.

Figures 4(a, b) illustrate the neural network results on the training and evaluation datasets, while Figure 4(d) reveals the error histogram in the time series. Observed and predicted values in the training and validation datasets are depicted in Figure 5. The correlation between the observed and predicted values in the training and validation datasets were 0.64 and 0.67, respectively.
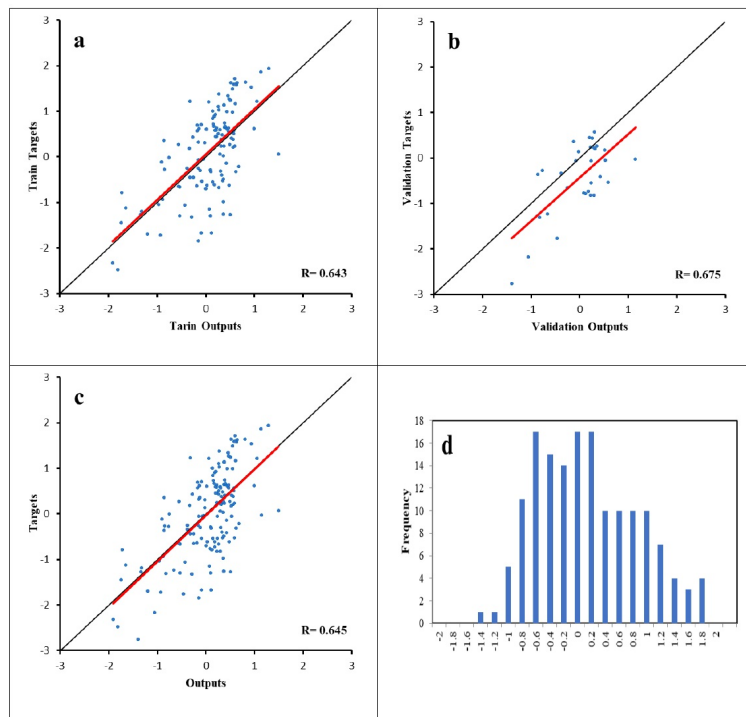

Figure 4: Neural network results in a) train dataset, b) validation dataset, c) All data, d) Error histogram of forecast
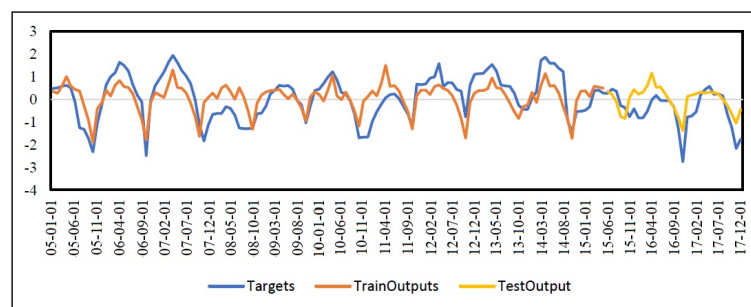

Figure 5: Time series of observed and predicted values in train and validation datasets.

Figure 4 illustrates that by incorporating proximity information from satellite images, model accuracy in the training and validation datasets was recorded as 0.643 and 0.675, respectively. Even though there was a decrease in accuracy during the training phase, a significant increase was observed during the validation phase. Furthermore, the error distribution seen in Figure 4(d) shows a reasonably uniform distribution around zero, with a significant reduction in error frequency.

The high accuracy of the wavelet neural network model can be attributed not only to the preprocessing and decomposition of the time series into sub-signals but also to the assignment of distinct weights for different sub-signals. Artificial neural networks are capable of modeling nonlinear behaviors; however, they struggle with accurately modeling non-stationary signals [29]. Given the non-stationary and nonlinear nature of the 6-month SPI time series, the application of the wavelet transform in the neural network assembly was deemed necessary. The wavelet transform substantially enhances model accuracy by generating multi-scale features by decomposing the original signal into high and low frequencies.

The findings indicated that employing adjoining information can result in more accurate drought forecasting than with the simple neural wavelet model alone. This is substantiated by Cannas et al. [8], who used a neural wavelet model to estimate monthly river flows in Italy, with results indicating that discrete wavelet preprocessing notably enhances the accuracy of neural network models.

The wavelet neural network model demonstrated acceptable accuracy in drought forecasting, thereby proving its potential for application in drought forecasting to facilitate improved water resource management and appropriate drought response decisions. The artificial intelligence technique, which employs satellite data in modeling and forecasting the SPI index, was found to be accurate.

4 Conclusion

Drought is one of the most devastating natural disasters and is currently affecting numerous countries. Remote sensing data can monitor most drought parameters, providing continuous spatial and temporal data. Nonlinear methods prove to be helpful in modeling and predicting this phenomenon better, given the nonlinear relationship of many drought parameters.

The precipitation condition and evapotranspiration condition indices are included among these drought parameters. Time series of these indices were generated using satellite products, and drought forecasting was executed using the hybrid wavelet neural network method.

The findings demonstrated that the wavelet neural network method could accurately forecast drought intensity for the subsequent year, as the R^2 value for 2016 was equal to 0.675. These findings further substantiated that artificial neural network algorithms are beneficial in forecasting the SPI drought index, and the usage of proximity information available in satellite data can enhance the accuracy of forecasts.

References

[1] M.A. Alawsi, S.L. Zubaidi, N.S.S. Al-Bdairi, N. Al-Ansari and K. Hashim, *Drought forecasting: a review and assessment of the hybrid techniques and data pre-processing*, Hydrology **9** (2022), no. 7, 115.

[2] L. Anastasakis and N. Mort, *The development of self-organization techniques in modelling: a review of the group method of data handling (GMDH)*, Research Report-University of Sheffield Department of Automatic Control and Systems Engineering, 2001.

[3] S.S. Band, I. Al-Shourbaji, H. Karami, S. Karimi, J. Esfandiari and A. Mosavi, *Combination of group method of data handling (GMDH) and computational fluid dynamics (CFD) for prediction of velocity in channel intake*, Appl. Sci. **10** (2020), no. 21, 7521.

[4] J. Bazrafshan and S. Hejabi, *Drought: Monitoring Methods*, University of Tehran Press, 2016.

[5] M. Behifar, A.A. Kakroodi, M. Kiavarz and G. Azizi, *Satellite-based drought monitoring using optimal indices for diverse climates and land types*, Ecolog. Inf. **76** (2023), 102143.

[6] A. Belayneh, J. Adamowski, B. Khalil and B.J.J.O.H. Ozga-Zielinski, *Long-term SPI drought forecasting in the Awash river basin in Ethiopia using wavelet neural network and wavelet support vector regression models*, J. Hydrol. **508** (2014), 418–429.

[7] D.H. Burn and N.K. Goel, *The formation of groups for regional flood frequency analysis*, Hydrological Sci. J. **45** (2000), no. 1, 97–112.

[8] B. Cannas, A. Fanni, G. Sias, S. Tronci and M.K. Zedda, *River flow forecasting using neural networks and wavelet analysis*, Geophys. Res. Abstr. **7** (2005), 08651.

[9] E.O. Center, *TRMM Data User's Handbook*, National Space Development Agency of Japan, 2001.

[10] S.D. Conte and C. De Boor, *Elementary numerical analysis: an algorithmic approach*, Society for Industrial and Applied Mathematics, 2017.

[11] S. Djerbouai and D. Souag-Gamane, *Drought forecasting using neural networks, wavelet neural networks, and stochastic models: Case of the Algerois Basin in North Algeria*, Water Resources Manag. **30** (2016), 2445–2464.

[12] I. Emadodin, T. Reinsch and F. Taube, *Drought and desertification in Iran*, Hydrology **6** (2019), no. 3, 66.

[13] A. Ghiami Bajgirani, M. Sharifi, M. Maghrebi and J. Arefi, *Applying Fourier and Wavelet transforms to extract instantaneous unit hydrograph*, Iran-Water Resources Res. **6** (2010), no. 2, 27–35.

[14] Z. Hao, V.P. Singh and Y. Xia, *Seasonal drought prediction: advances, challenges, and future prospects*, Rev. Geoph. **56** (2018), no. 1, 108–141.

[15] H. Iba, H. DeGaris and T. Sato, *A numerical approach to genetic programming for system identification*, Evol. Comput. **3** (1995), no. 4, 417–452.

[16] A.G. Ivakhnenko, *Polynomial theory of complex systems*, IEEE Trans. Syst. Man, Cybernet. **4** (1971), 364–378.

[17] H. Khedmati, M. Manshouri, M. Heydarizadeh and H. Sedghi, *Zonation and estimation of flood discharge in unguaged sites located in south-east basins of Iran using a combination of flood index and multi-variable regression methods*, J. Water Soil **24** (2010), no. 3, 593–609.

[18] A.S. Kiem, F. Johnson, S. Westra, A. van Dijk, J.P. Evans, A. O'Donnell, A. Rouillard, C. Barr, J. Tyler, M. Thyer and D. Jakob, *Natural hazards in Australia: droughts*, Climatic Change **139** (2016), 37–54.

[19] T.W. Kim and J.B. Valdés, *Nonlinear model for drought forecasting based on a conjunction of wavelet transforms and neural networks*, J. Hydrol. Eng. **8** (2003), no. 6, 319–328.

[20] R.J.E. Merry and M.J.G. van de Molengraft, *Wavelet Theory and Applications: A Literature Study*, Eindhoven University of Technology Department of Mechanical Engineering Control Systems Technology Group, 2005.

[21] A.K. Mishra and V.P. Singh, *Drought modeling–A review*, J. Hydrol. **403** (2011), no. 1–2, 157–175.

[22] V. Nourani, M. Komasi and A. Mano, *A multivariate ANN-wavelet approach for rainfall–runoff modeling*, Water Resources Manag. **23** (2009), no. 14, 2877–2894.

[23] A. Pahlavanroy, H. Ghasemi and M. Afshari, *Investigating the drought trend of Isfahan province with SIAP statistical index*, Fifth Nat. Conf. Watershed Manag. Sci. Engin. Iran, Gorgan, 200).

[24] W. Pozzi, J. Sheffield, R. Stefanski, D. Cripe, R. Pulwarty, J.V. Vogt, R.R. Heim, M.J. Brewer, M. Svoboda, R. Westerhoff and A.I. Van Dijk, *Toward global drought early warning capability: Expanding international cooperation for the development of a framework for monitoring and forecasting*, Bull. Amer. Meteorol. Soc. **94** (2013), no. 6, 776–785.

[25] J. Schmidhuber, *Deep learning in neural networks: An overview*, Neural Networks **61** (2015), 85–117.

[26] S. Shaghaghi, H. Bonakdari, A. Gholami, I. Ebtehaj and M. Zeinolabedini, *Comparative analysis of GMDH neural network based on genetic algorithm and particle swarm optimization in stable channel design*, Appl. Math. Comput. **313** (2017), 271–286.

[27] W. Wei, J. Zhang, L. Zhou, B. Xie, J. Zhou and C. Li, *Comparative evaluation of drought indices for monitoring drought based on remote sensing data*, Environ. Sci. Pollution Res. **28** (2021), no. 16, 20408–20425.

[28] D.A. Wilhite, *Preparing for drought: A methodology*, Drought: A Global Assessment, Vol. II, edited by Donald A. Wilhite, chap. 35, London: Routledge, 2000, pp. 89—104.

[29] M. Younesi, N. Shahraki, S. Marofi, H. Nozari, *Drought forecasting using artificial wavelet neural network integrated model (WA-ANN) and time series model (ARIMA)*, Irrig. Sci. Eng. **41** (2018), no. 2, 167–181.

[30] Y. Zhang, *PML_V2 Global Evapotranspiration and Gross Primary Production (2002.07-2019.08)*, National Tibetan Plateau Data Center, 2020.

[31] A. Zhang and G. Jia, *Monitoring meteorological drought in semiarid regions using multi-sensor microwave remote sensing data*, Remote Sens. Envir. **134** (2013), 12–23.